Deformable Mirrors for High-Power Lasers

Supriyo Sinha[*a], Justin D. Mansell[**b], and Robert L. Byer[a]
[a]Ginzton Laboratory, Stanford University; [b]Intellite, Inc.

ABSTRACT

We describe the performance of a bulk micromachined deformable mirror coated with a dielectric stack for adaptive optics applications with high power lasers. A reflectance of greater than 99.9% was measured and the mirror had a residual static aberration of less than 90 nm rms primarily in astigmatism. A thermally induced distortion of 71 nm RMS was observed for an incident intensity of 300 W/cm^2 and an average power of 57 W. The multi-layer coated deformable mirror survived over half a billion cycles without degradation and survived for 30 hours with 36 W cw 1064 nm laser light. In addition, the thermally induced distortion with 22 W of average laser power (350 W/cm^2) was reduced from 88 nm to 31 nm rms.

Keywords: deformable mirrors, lasers, adaptive optics, high-power, thermal loading, LIGO, multi-layer dielectric

1. INTRODUCTION

Gravitational wave interferometry requires great sensitivity to detect effective arm length changes on the order of 10^{-20} m induced by gravitational waves. The Laser Interferometer Gravitational-Wave Observatory (LIGO) was designed to be maximally sensitive to gravitational wave radiation.[1] Figure 1 shows a simplified version of the optical setup used by LIGO. To achieve such sensitivity, the effects of all relevant noise sources were minimized and the laser power entering the interferometer should be maximized. A master oscillator laser illuminates a series of laser amplifiers and conditioning optics like lenses, a Faraday isolator, and an electro-optics modulator (EOM) before the Fabry-Perot ring mode cleaner. The mode cleaner is tuned to filter the laser so that only the lowest order Hermite-Gaussian laser mode is transmitted and laser power in the higher-order transverse modes is reflected.

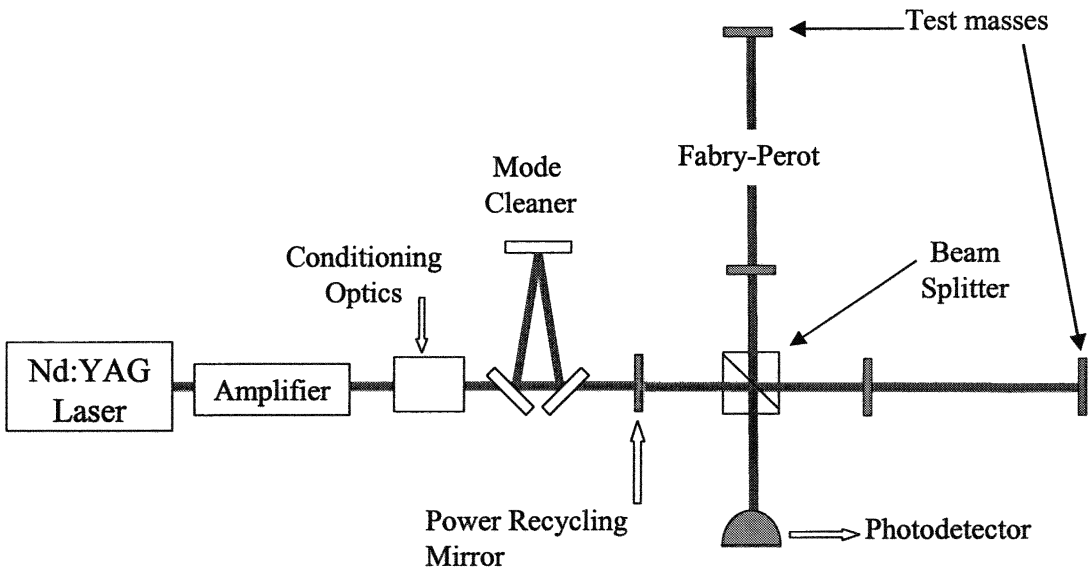

Figure 1 - Simplified optical schematic of the Laser Interferometer Gravitational-Wave Observatory (LIGO).

[*]supriyo@stanford.edu; phone 1 650 725-2266; fax 1 650 725-2666; http://www.stanford.edu/~supriyo; Stanford University, 450 Via Palou, Stanford, CA, USA 95305; [**]jmansell@intellite.com; phone 1 505 268-4742; fax 1 505 268-4741; http://www.intellite.com; Intellite, Inc., 1717 Louisiana Ste. 202, Albuquerque, NM, USA 87110

High-Resolution Wavefront Control: Methods, Devices, and Applications III, John D. Gonglewski, Mikhail A. Vorontsov, Mark T. Gruneisen, Editors, Proceedings of SPIE Vol. 4493 (2002)

Unfortunately aberrations induced by absorption of laser light in the conditioning optics and in the non-uniform thermal field in the laser amplifier cause light to be rejected from the mode cleaner.[2] We proposed to put an adaptive optics (AO) system in the optical system before the mode cleaner to compensate the aberrations induced in the laser amplifier and the conditioning optics and maximize the laser power available for gravitational wave detection. The spatial phase correcting element in such an adaptive optics system must be able to handle the 200W of laser power proposed for LIGO II. This paper discusses the performance of a continuous membrane micro-machined deformable mirror coated with a multi-layer dielectric (MLD) stack.

2. MIRROR ARCHITECTURE

It is difficult to find a spatial phase control element that lends itself well to handling high-power laser light. Liquid crystal spatial phase modulators are unsuitable for handling high laser power because their absorbing indium tin oxide (ITO) transparent electrodes damage easily. Multi-layer dielectric-coated deformable mirrors are much more promising in handling high laser powers. Traditional lead magnesium niobate (PMN) actuated mirrors are difficult to coat with a MLD stack because they lack the structural rigidity to counteract the stress induced by the coating.[3] Segmented mirrors are also undesirable in this application due to diffractive effects and the potential for damage on the edges of the mirrors. Surface micro-machined deformable mirrors suffer from poor surface quality due to the surface perforations that are used during wet release.[4] These perforations create areas of high absorption that can cause permanent damage when used with high intensity lasers.

Traditional bulk-micromachined mirrors have truly continuous surfaces, but the surfaces of most bulk-micromachined mirrors are exposed only after wet etching.[5] A surface of silicon nitride exposed during wet etching runs the risk of suffering from high scatter loss due to interaction of the etchant with the mirror surface. Furthermore, generating the mirror surface with wet etching prevents the dielectric coating from being deposited on the mirror until all the processing has been done which increases the likelihood of static aberrations since the mechanical stability of the wafer is not available during coating runs. In addition, most bulk-micromachined deformable mirror architectures suffer from high crosstalk between actuators, a disadvantage also shared by bimorph deformable mirrors.

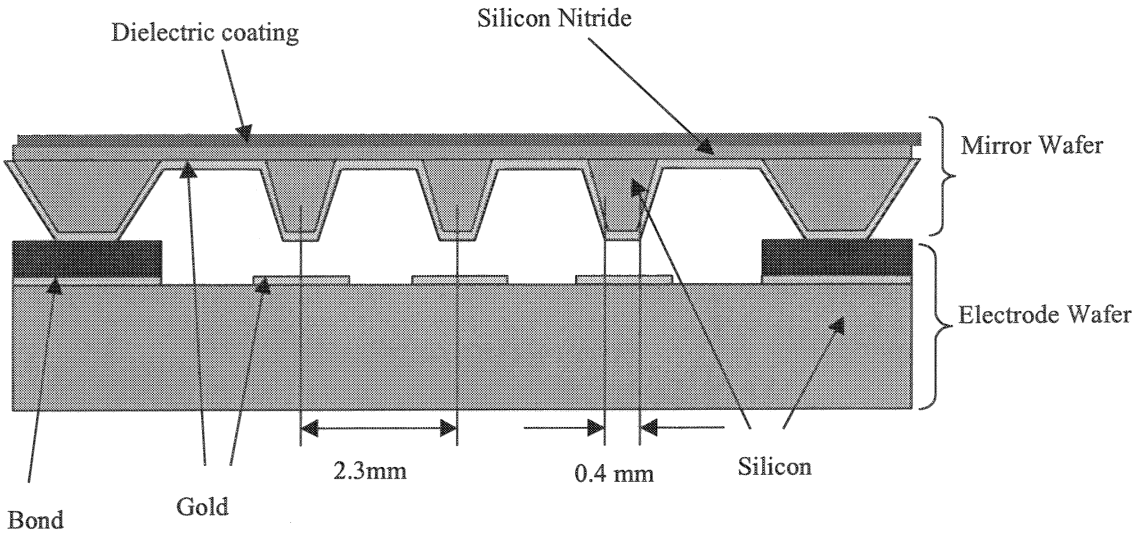

Figure 2 - Cross-sectional view of the deformable mirror architecture.

Figure 2 shows a cross-sectional view of the deformable mirror architecture we designed for high-power lasers. Our initial primary concern with this architecture was the preservation of the mirror surface. This deformable mirror

architecture can be coated before processing when processed with a one-sided etcher formed with o-rings and a Teflon or polypropylene mechanical container. The mirror surface is formed from one of the nitride coated polished sides of the wafer. Since the mirror surface is not formed by etching, the dielectric coating can be deposited onto the nitride before any processing steps are taken.

We fabricated a 19 actuator, 16 mm diameter deformable mirror with this architecture. The rms static distortions before and after bonding to the electrode wafer were 30 nm and 100 nm respectively. The pillars illustrated in the above architecture are approximately 400 μm high with 400 μm diameter tips and 76-degree sidewalls.

3. COATING EVALUATION

Figure 3 is a photograph of the deformable mirror coated with an 8 layer dielectric stack designed for 99.9% reflectivity when used at normal incidence with 1064nm light. The vendor also quoted an absorption value of 20 ppm at 1.06 μm. The transmittance of the coating was experimentally verified by measuring the transmitted power of a 300 mW non-planar ring oscillator (NPRO) versus incident power. Care was taken to ensure that the beam did not pass through any of the silicon pillars, since silicon strongly absorbs at this wavelength. A transmittance of 0.07% was measured, which, if scattering is assumed to be negligible and the quoted value of absorption is used, corresponds to a reflectance of 99.93%.

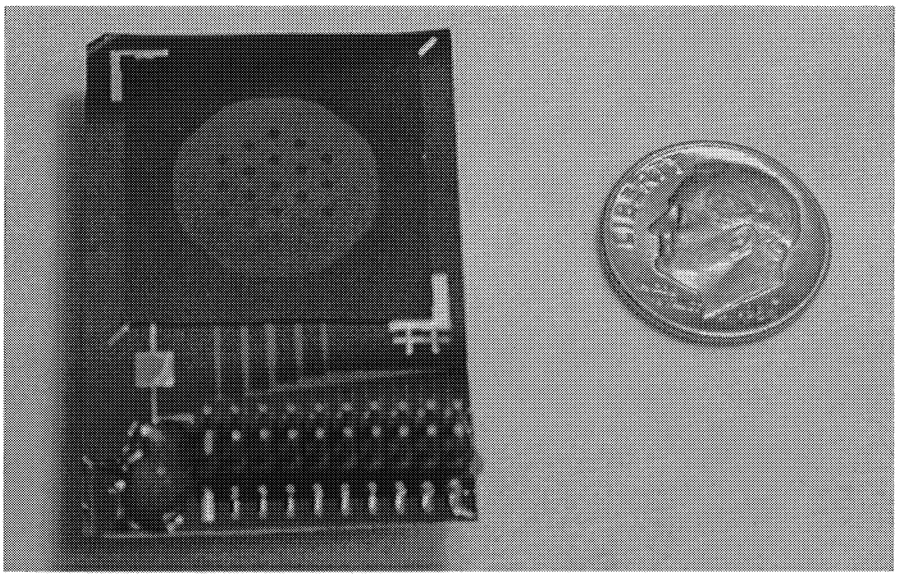

Figure 3 - Photograph of the deformable mirror coated with a multi-layer dielectric stack.

We measured the static aberrations with a Hartmann wavefront sensor. The dielectrically coated deformable mirrors had an rms static distortion of 89.5 nm, which is approximate 1/12 λ at 1.06 μm. The distortion was mainly in astigmatism distributed across the mirror surface. Figure 4 shows three influence functions measured with the Hartmann wavefront sensor. The images show that the influence functions are fairly localized. At a voltage of 150 V, the mirror had a throw of about 3 μm.

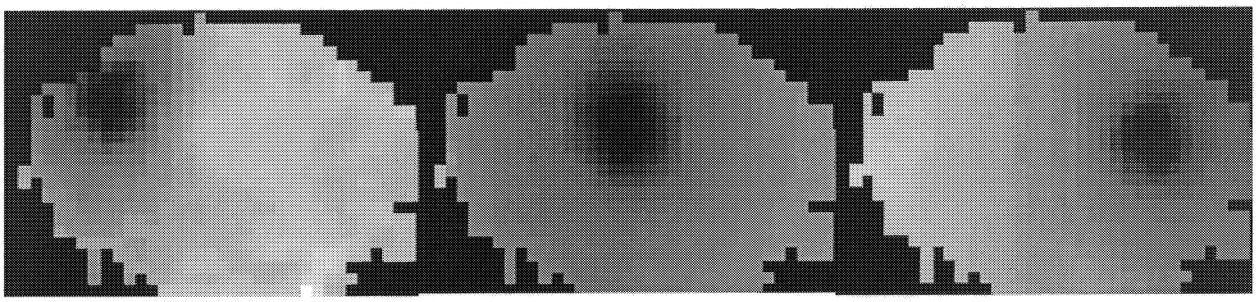

Figure 4 - Three false-color images of the influence functions of the dielectric deformable mirror measured with a Hartmann wavefront sensor.

4. THERMAL DISTORTION MEASUREMENTS

4.1 Thermal loading of gold coated deformable mirror

We first thermally loaded a deformable mirror with no dielectric high reflector stack. This mirror had a 200 nm gold coating instead of the dielectric coatings. Figure 5 shows the experimental setup to thermally load the mirror and measure the thermally induced distortion. We built a multi-mode laser from a 3:1 aspect ratio Nd:YAG laser slab, a high reflectivity mirror, a 100 mm focal length lens, and a 22% output coupler. The output of the Nd:YAG laser was imaged onto the deformable mirror. The beam spot on the deformable was a rectangular image of the rectangular slab aperture. Using a rotating scanning slit, the beam width and height were measured to be 9.2 mm and 2.1 mm respectively. The intensity profile of the beam in the vertical dimension was nearly gaussian, but in the horizontal dimension the beam was more top-hat due to the higher-order transverse modes. A helium-neon (HeNe) laser at 633 nm was expanded to illuminate the deformable mirror. The HeNe laser was used to probe the deformable mirror surface during the experiment. A 1064 nm high reflectivity dielectric mirror was placed before the wavefront sensor to reject stray 1064nm laser light. The surface of the deformable mirror was imaged onto the wavefront sensor at a magnification of 0.6. Output power of the resonator was measured with a flipper mirror (placed between the 22% output coupler and the 150 mm lens) and a thermal power meter.

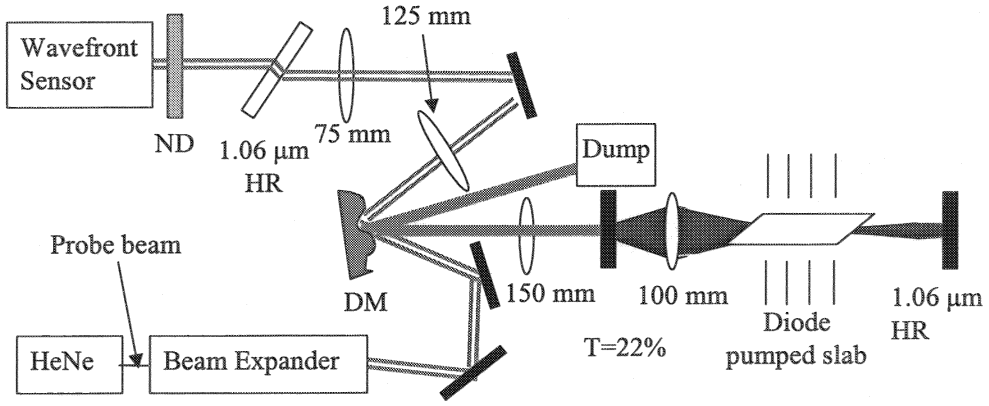

Figure 5 - Optical setup used to thermally load the deformable mirror.

With 27 W of cw 1064nm laser power on the deformable mirror, an rms distortion of 32.3 nm was measured. With 41 W of laser power on the deformable mirror, an rms distortion of 39.1 nm was measured. Figure 6 shows the measured wavefront distortion and the wavefront slopes at 41 W incident power. The corresponding intensity for this power level is 212 W/cm^2. An examination of the measured wavefront and wavefront tilts shows that the distortions appear to be particularly concentrated about the pillars of the deformable mirror. One possible cause of this type of distortion is the

differential thermal expansion of the silicon pillars and the silicon nitride membrane. Another possible cause is that the different thermal properties of the pillared and non-pillared areas result in a spatial temperature distribution over the deformable mirror surface.

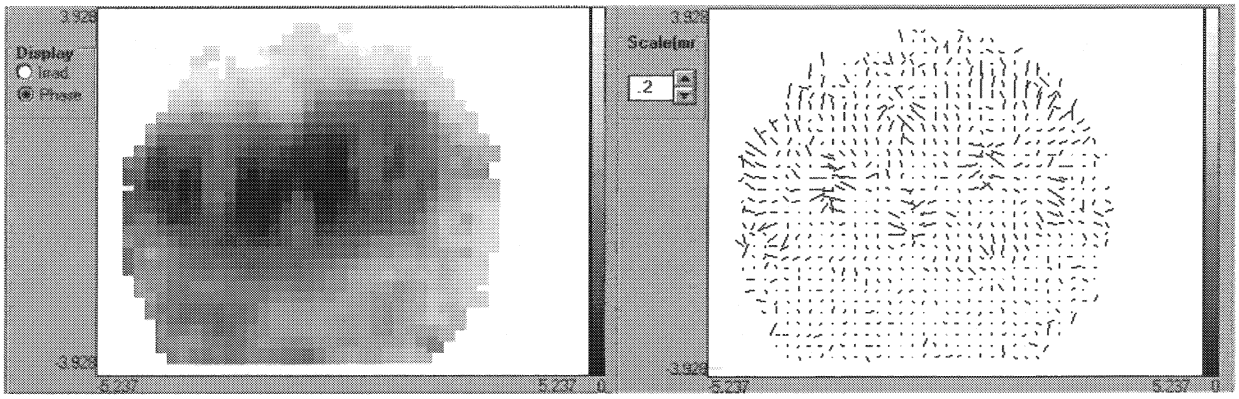

Figure 6 - False color image of the wavefront distortion and the wavefront slopes measured by the Hartmann wavefront sensor when illuminating the gold-coated deformable mirror with 41W of cw 1064nm laser power.

4.2 Thermal loading of dielectric coated wafer

We next thermally loaded a 4" wafer that had been coated with the dielectric stack but had not undergone any processing. The wafer was placed inside a laser cavity so that it could be thermally loaded with high laser power. Figure 7 shows the experimental setup used to test the MLD-coated wafer. The curved 1.06 μm high reflector end-mirror in the cavity actually had a measured transmittance of 0.17%; measuring the power through this mirror permitted easy calculation of the circulating power in the cavity. Using an imaging system and a rotating scanning slit, the dimensions of the YAG beam on the mirror was measured to be 1.03 mm in the vertical dimension and 2.76 mm in the horizontal dimension. The beam was very rectangular and had nearly the same aspect ratio as the Nd:YAG slab.

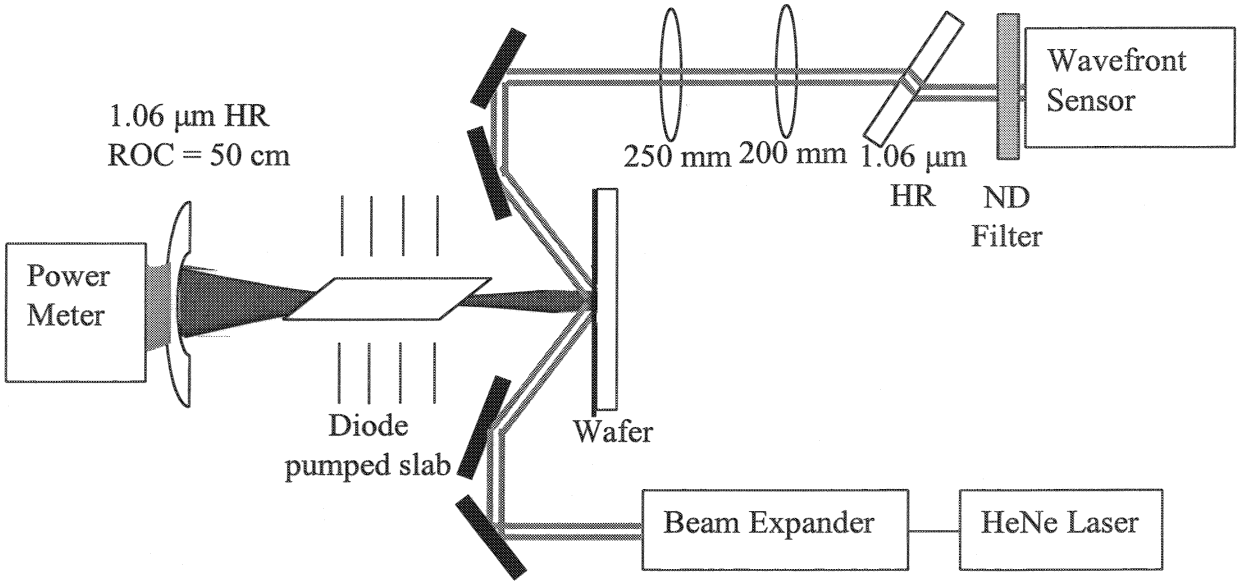

Figure 7 - Experimental setup used to test the thermally induced distortions of an MLD-coated silicon wafer as one of the mirrors of the laser resonator.

Increasing the diode pump power to the slab allowed us to achieve circulating powers up to 1.1 kW, which corresponds to an intensity of 38.7 kW/cm^2 on the surface of the wafer. Even at these high intensities, no distortion was measurable with the wavefront sensor. The wavefront sensor used had an rms resolution of approximately 10 nm, or one hundredth of a wave at 1.06 μm.

4.3 Thermal loading of dielectric coated deformable mirror

After observing the effects of thermally loading the wafer, we replaced the gold-coated deformable mirror in Figure 5 with the deformable mirror coated with a multi-layer dielectric stack. In addition we also replaced the HeNe probe laser with a 1.06 μm wavelength NPRO since the amount of 633 nm light reflected from a given portion of the surface of the dielectrically coated deformable mirror depends on whether or not a pillar lies directly underneath the surface. Beam tubes were used to prevent the diode-pumped slab laser light from entering the wavefront sensor.

We thermally loaded the mirror and noticed thermally induced distortions at powers above 15 W. At 41 W, the rms distortion was 61.3 nm; at 57 W, the rms distortion was 86.8 nm. Figure 6 shows the distortion of the wavefront of the reflected HeNe probe beam for 41 W of 1064 nm cw laser power. The corresponding intensity for this power level is 212 W/cm^2.

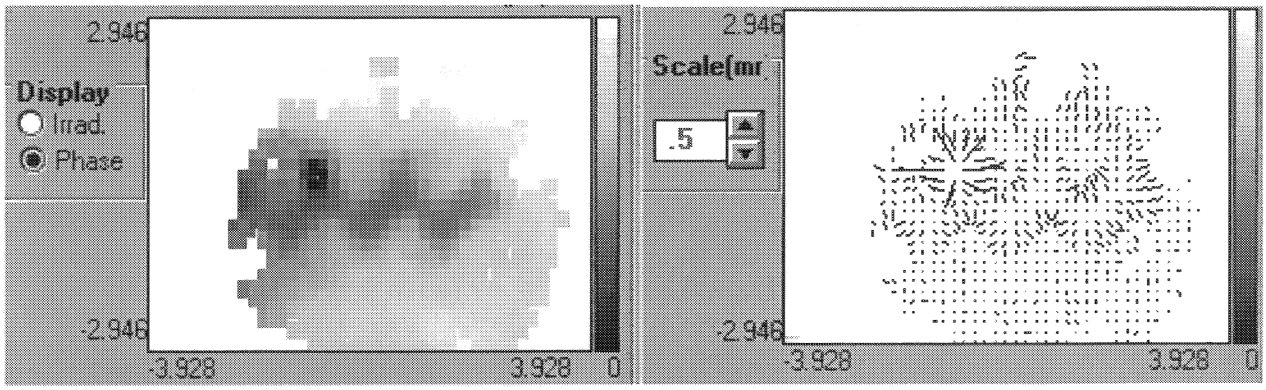

Figure 8 - Measured wavefront distortion induced by thermally loading the MLD-coated deformable mirror with 41 W of cw 1064nm laser power.

The distortions are again primarily concentrated around the edge of the pillars, similar to the thermally induced wavefront distortions observed with the gold-coated deformable mirror. Again one possible cause of this is the differential thermal expansion of the silicon pillars and the silicon nitride membrane. Another possible cause is the fact that after light passed through the silicon nitride, it either illuminated the silicon pillars or the chrome sticking layer used in the gold coating. The chrome coating would reflect most of the incident light, while the silicon would absorb most of the light, thus creating a non-uniform temperature profile.

4.4 Thermally induced distortion mechanisms

We next tried to understand the mechanisms of the thermally induced distortions. As said earlier, one possible explanation is that the high laser power creates a spatially varying temperature distribution, which may warp the surface because different portions of the nitride membrane would expand differently according to the local temperature. A non-uniform temperature distribution in the membrane could occur if the silicon pillars act as very efficient radiators causing local cooling, with the result that the nitride at the base of pillars is cooler than the surrounding nitride. In this case, the surrounding nitride would be heated up due to the absorption in the chrome gold layer on the backside of the membrane. To experimentally determine if that was the case, a MLD-coated deformable mirror without gold on the backside was thermally loaded. The nitride at the base of the pillars of these mirrors must be hotter than the surrounding nitride since there is no chrome-gold to absorb the light. The experiment showed that the distortions were of the same nature and of the same magnitude as the backside gold-coated dielectric stack deformable mirror. Thus, it was concluded that the nitride underneath the base of the pillars could not be cooler than the surrounding nitride.

A spatial thermal distribution could also occur if the silicon pillars are absorbing much more heat than the non-pillared areas, causing the nitride underneath the base of the pillars to be hotter than the surrounding nitride. This could cause

the thermal distortions seen in the DM, since the nitride on different portions of the membrane would expand according to the local temperature.

Another possible source of the thermally induced distortions is the differential thermal expansion of the silicon nitride at the base of the pillars and the silicon pillars themselves. In this case, the distortion would be caused by differences in the thermal expansion coefficient of silicon and silicon nitride. Silicon's thermal expansion co-efficient is lower than that of silicon nitride by approximately 0.6 ppm/C.[6] This effect would explain the localization of the deformations at the edge of the pillars, since it is only at the edges of the pillars that the silicon and silicon nitride are of comparable thickness.

To try to remove the effect of differential thermal expansion between the silicon and the silicon nitride, we fabricated an all-silicon deformable mirror architecture. Instead of etching the non-pillared section of the silicon completely down to the nitride, the etch was stopped when approximately 50 μm of silicon remained and the nitride was completely removed from the structure. We built a wafer of these all-silicon deformable mirror architectures with measured silicon thickness in the non-pillared area of 55 μm. We deposited on the surface of some of the mirrors 200 nm of gold for reflectivity. The other mirrors remained uncoated structures. Both the gold-coated and bare silicon mirrors showed approximately ten waves of parabolic distortion due to the fact that there is no tension in the single-crystal silicon.

The gold-coated all-silicon mirror was evaluated in the setup described in Figure 5. Even with 55 W of 1064 nm laser power (approximately 300 W/cm^2), no distortion was observed in the mirror. Since we are not interested in the quantitative power handling of this structure, but rather how the mirror distorts when under severe thermal load, the gold-coated mirror was replaced with the bare silicon mirror. At 7 W of incident power (approximately 35 W/cm^2), severe thermally induced distortions were seen. The resulting wavefront slopes are given below in Figure 9.

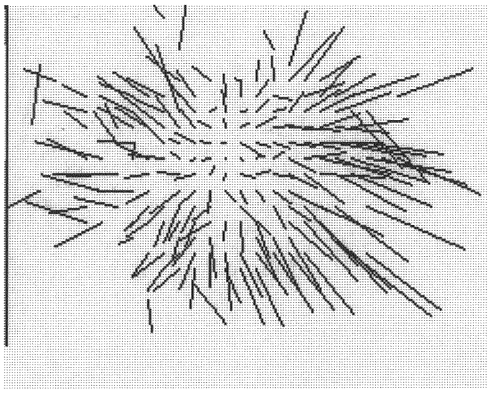

Figure 9 - Wavefront slopes measured when loading the all-silicon deformable mirror structure with 7 W of cw 1064 nm laser power.

The above figure corresponds to an rms distortion of 450 nm, but the distortion is not concentrated around the pillars but about the whole area of the beam. This is despite the fact that a significant non-uniform spatial thermal field should still exist. This strongly suggests that differential thermal expansion is the main cause of the thermal distortions seen in the silicon nitride deformable mirror structures. However, before such a conclusion can be confidently reached, further tests will be performed with thinner all-silicon structures.

5. MIRROR DAMAGE THRESHOLD MEASUREMENTS

In addition to assessing the dielectrically-coated deformable mirror's flatness and thermally induced distortions, tests were also done on the deformable mirror's damage threshold and robustness. The deformable mirror was placed inside the laser resonator, like in Figure 7. The deformable mirror suffered permanent damage at a laser intensity of 25 kW/cm^2. Figure 10 shows the permanent measured by the Hartmann wavefront sensor. Visual inspection of the damaged deformable mirror revealed that the damage occurred at a pillar. Thus, it is reasonable to assume that poor thermal extraction is the cause of damage. We believe that the increased mirror temperature caused annealing to occur in the mirror and thus permanent damage.

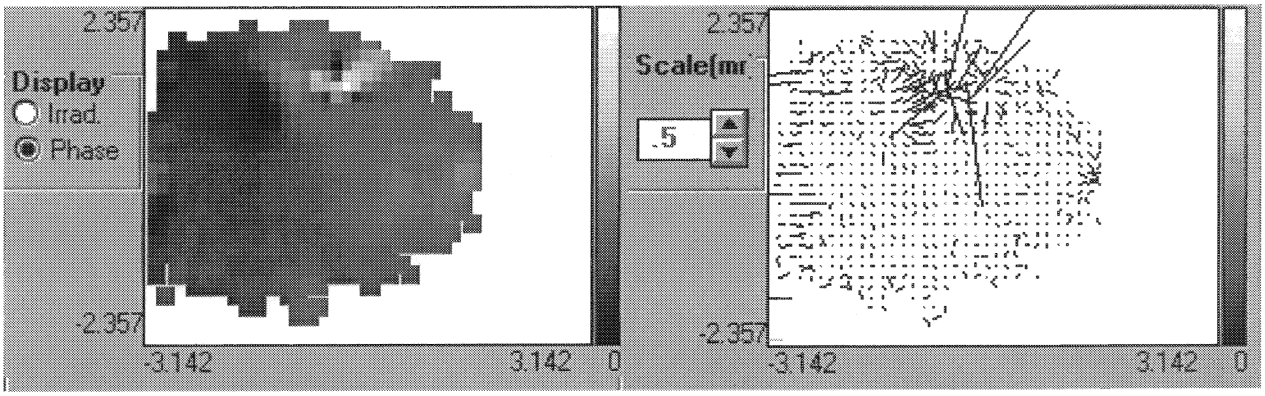

Figure 10 - Wavefront distortions permanently induced on a deformable mirror after recieving 25kW/cm^2 of cw 1064nm laser radiation inside a laser resonator.

6. LONG-TERM DURABILITY

We also wanted to determine how well the dielectric stack held to the nitride membrane during actuation and if cycling the actuators for a long period of time would distort the coating. We cycled the actuators at 150 V for over half a billion cycles with no observed deterioration in surface quality.

In addition to cycling the actuators, we also wanted to measure any degradation in the mirror coating after being hit with a considerable amount of continuous laser power for long periods of time. We put 36 W of continuous wave laser power (an intensity of 187 W/cm^2) onto the mirror surface for over 30 hours. Neither the Michelson interferometer nor the wavefront sensor observed any degradation.

7. ACTIVE THERMAL ABERRATION COMPENSATION

Although the presence of thermally induced distortions are undesirable, it would be of advantageous if the deformable mirror could statically compensate for these distortions. The major disadvantage of using the deformable mirror to compensate for the thermal distortions on its own surface is reduced available throw to correct for dynamic aberrations in the laser system, but this penalty is not as serious as the inability to compensate for thermal distortions.

We used the experimental setup shown in Figure 5, but replaced the 150 mm lens with a 50 mm lens to increase the 1064 nm laser intensity on the deformable mirror. Continuous laser power of 22 W corresponding to an intensity of 350 W/cm^2 incident on the static deformable mirror produced a thermally induced distortion of 88 nm rms. We used a genetic searching algorithm was used to search for a set of actuator voltages that would minimize this induced distortion. After 20 generations of the genetic algorithm, the rms wavefront error was reduced from 88 nm to 31 nm.

8. CONCLUSIONS

We presented here an evaluation of a micromachined membrane deformable mirror with several different types of high reflectivity coatings. In our measurements, we found that thermally induced deformation was concentrated at the edges of the pillars, suggesting either a spatially varying temperature profile or a differential thermal expansion between the silicon pillars and the silicon nitride membrane. We created an all-silicon mirror structure to eliminate the possibility of differential thermal expansion and found that unlike the silicon nitride deformable mirrors, thermally-induced distortions in the all-silicon structure were not concentrated at the pillar edges. We plan to investigate measuring the temperature of the deformable mirror to determine the existence and nature of the spatially varying thermal field in the silicon nitride implementation of the architecture.

ACKNOWLEDGEMENTS

We thank the National Science Foundation for funding this work via the LIGO development effort. We also thank Patrick Lu for helping with some of the deformable mirror fabrication.

REFERENCES

[1] A. Abramovici, W. E. Althouse, R. W. P. Drever, Y. Gursel, S. Kawamura, F. J. Raab, D. Shoemaker, L. Sievers, R. E. Spero, K. S. Thorne, R. E. Vogt, R. Weiss, S. E. Whitcomb, and M. E. Zucker. "LIGO: The Laser Interferometer Gravitational-Wave Observatory", *Science* **256**, pp. 325-33, 1992.

2 J. D. Mansell, J. Hennawi, E. K. Gustafson, M. M. Fejer, R. L. Byer, D. Clubley, S. Yoshida, D. H. Reitze. "Evaluating the effect of transmissive optic thermal lensing on laser beam quality with a Shack-Hartmann wave-front sensor", *Applied Optics*; **40**, 3, pp. 366-74, 2001.

[3] M. A. Ealey. "Active and adaptive optical components: a general overview", *Proceedings of the ADPA/AIAA/ASME/SPIE Conference*, pp. 781-4, 1991.

[4] T. Bifano, J. Perreault, and P. Bierden. "A micromachined deformable mirror for optical wavefront compensation", SPIE Vol. 4124, pp. 7-14, 2000.

[5] L.M. Miller, M.L. Argonin, R.K. Bartman, W.J. Kaiser, T.W. Kenny, R.L. Norton, E.C. Vote. "Fabrication and characterization of a micromachined deformable mirror for adaptive optics applications", SPIE Vol. 1945, pp. 421-430, 1993.

[6] Rauschert Technical Ceramics, http://www.rauschertus.com/technical_ceramics/silicon_nitride.html, cited on July 24, 2001.